PHYSICAL REVIEW C **81**, 034612 (2010)

Strong coupling effects in proton scattering from ^{8}He

R. S. Mackintosh*
Department of Physics and Astronomy, The Open University, Milton Keynes, MK7 6AA, United Kingdom

N. Keeley†
Department of Nuclear Reactions, The Andrzej Sołtan Institute for Nuclear Studies, Hoża 69, PL-00681, Warsaw, Poland
(Received 15 September 2009; revised manuscript received 20 February 2010; published 31 March 2010)

We present dynamic polarization potentials (DPPs), due to both neutron and neutron-pair pickup coupled reaction channels, contributing to the proton-nucleus interaction for the case of ^{8}He at 15.66, 25, and 61.3 MeV/nucleon. The available elastic scattering and transfer data were fitted in coupled reaction channels calculations that allowed full interpartition couplings. In addition, the contributions with various different combinations of coupled reaction channels were considered; we show that this can throw light on the nonlocality of the underlying DPP, for which we determine the local and L-independent equivalent.

DOI: 10.1103/PhysRevC.81.034612 PACS number(s): 25.70.Bc, 25.70.Hi, 24.10.Eq

I. INTRODUCTION

It has been known for some time that the coupling to deuteron channels makes an important contribution to proton scattering and can significantly improve the fit to certain data. The earlier coupled reaction channel (CRC) calculations [1–4] omitted nonorthogonality terms [5,6] but computational developments have more recently allowed them to be included. The development of inverse scattering techniques, whereby the potential that yields a specific S matrix S_{lj} can reliably be calculated [7], makes it possible to determine a local potential that represents the coupling effects. That is, we can find a local single channel potential that precisely reproduces all details of the elastic scattering as calculated by the full CRC formalism. Such potentials are of interest for comparison with pure phenomenologically fitted potentials and with potentials derived by folding models. A consistent finding [8,9] of the earlier work was that deuteron channels contribute a significant *repulsive* component to the nucleon-nucleus interaction, in addition to the expected absorptive component. The induced potential, the dynamical polarization potential (DPP), is never proportional to the bare potential so the coupling effects cannot be represented as a renormalization of it.

Recent work [10], including nonorthogonality corrections, confirms the repulsive effect of the contribution of the ^{8}He$(p,d)^{7}$He pickup reaction to $p+{}^{8}$He elastic scattering at a bombarding energy of 15.66 MeV/nucleon and finds very strong additional absorption. Although nonorthogonality corrections significantly modified the details of the DPP, the qualitative features were consistent with earlier findings. A subsequent study [11] involving pickup from ^{10}Be, a less atypical nucleus, also found repulsion as well as absorption. The absorption generated by ^{10}Be$(p,d)^{9}$Be coupling was less than for ^{8}He$(p,d)^{7}$He, but the imaginary part of the DPP also had a remarkable emissive region for $r \leqslant 2$ fm, suggestive of strong nonlocality and possibly L dependence. Effects such as this make it unrealistic to correct a folding model potential by uniformly renormalizing the real and imaginary parts, as is commonly done. Indeed, the potentials extracted by inversion from CRC calculations have properties that would not arise naturally from any folding procedure based on a local density model. This is consistent with the fact that precision fits to precise and wide-range elastic-scattering data often show evidence of such effects.

The nucleon-nucleus interaction is fundamental to nuclear physics, so we need to establish such properties of the pickup DPP as its dependence on energy and the nature of the target nucleus. The continued development of CRC calculations [5,6] affords us the opportunity to study the contribution of (p,d) coupling, alone or together with other reaction channels; in the present work we include coupling to the $t+{}^{6}$He channels. Various combinations of different reaction channels are defined in Sec. IV. This work provides the first evaluation of the magnitude and energy dependence of the DPP arising from two-nucleon pickup.

The calculations are carried out at three energies for which there is elastic-scattering data: 15.66, 25, and 61.3 MeV/nucleon. The present work extends, with a different emphasis, previous calculations [12] at 15.66 MeV/nucleon and 61.3 MeV/nucleon for which fits for the (p,d) and (p,t) angular distributions were published. We shall show that different contributions to the overall DPP vary with energy in sharply different ways related to angular-momentum matching. The combination of different reaction channels will be made to throw light on the nature of the underlying nonlocality of the channel-coupling contribution to the DPP, particularly its energy dependence. This nonlocality is very different to that associated with knock-on exchange and described phenomenologically by Perey and Buck [13]. Perey-Buck nonlocality, while very important, is certainly not, as seems sometimes to be assumed, the only form of nonlocality that is important for nuclear scattering.

Pickup coupling presents a challenge to elaborate theories of nucleon-nucleus interactions that do not include it explicitly. Thus, it is important to establish the contribution of reaction channels unambiguously. In support of the validity of the

*r.mackintosh@open.ac.uk
†keeley@fuw.edu.pl

CRC framework that underlies our results, we note that the same formalism and numerical procedures successfully explain the threshold anomaly in heavy ion scattering [14,15]. Although, for nucleon scattering, reaction channel coupling does not so clearly correspond to a previously recognized anomaly, the effects are not less in magnitude, implying that such coupling is a part of the nucleon-nucleus interaction that cannot be ignored. Even if an averaged, local, and L-independent representation of reaction channel effects is implicit within microscopic folding theories, their explicit inclusion is essential for precise fits for specific target nuclei.

The DPPs we present are determined by applying the iterative perturbative (IP) S_L to $V(r)$ inversion procedure [7] to S matrices calculated using the CRC method: the "CC-plus-inversion" procedure. Other means of calculating the DPP exist, and our brief overview of them will be drawn on when we discuss our conclusions, particularly concerning the effects of nonlocality. Since we include both coupled reaction channels (CRC) and continuum discretized coupled channels (CDCC), representing breakup in certain coupled partitions, we simply refer to coupled-channels (CC) calculations.

Section II reviews the deceptively slippery concept of the DPP. Section III reviews the many alternative ways in which it has been determined, with some account of their advantages and disadvantages, together with a specification of the method we have employed. Section IV gives a full specification of the CC calculations carried out, including details of the parameters employed and fits to the data. Section V presents details of the DPPs for all the different CC calculations at the three energies studied. In Sec. VI we describe the extent to which our general findings depend on the choices of various parameters that enter into our calculations. Section VII discusses the nonlocality of the DPP and the light thrown on this property by the results of Sec. V and Sec. VIII summarizes the findings, discusses the general implications for understanding nucleon-nucleus interactions, and notes certain directions in which the present work should be followed up.

II. THE DYNAMIC POLARIZATION POTENTIAL

A formal approach to calculating the DPP follows from the reaction theory of Feshbach [16], relevant parts of which are reviewed in subsection II A. Many articles write down an equation for the nucleon-nucleus or nucleus-nucleus interaction $V_{\rm OM}(r)$ of the form

$$V_{\rm OM}(r) = V_{\rm FM}(r) + V_{\rm DPP}(r) \tag{1}$$

in which expressions for the folding model (FM) potential $V_{\rm FM}(r)$ and the dynamic polarization potential (DPP) $V_{\rm DPP}(r)$ are either given or referenced, see, e.g., Ref. [17]. The FM potential typically depends only on the densities of the interacting nuclei and an effective nucleon-nucleon interaction (assuming double folding) which may depend on the nuclear densities and the asymptotic energy, E. In general, it will depend smoothly on N, Z, and E. Strictly, $V_{\rm FM}(r)$ is nonlocal as a result of exchange processes (Fock term), though, for elastic scattering, a local equivalent potential is generally used. Due to the Perey effect [18], this local potential is not equivalent for nonelastic processes, although this becomes less significant as the mass number of the projectile increases [19]. We emphasize that exchange nonlocality is *not* the same as the nonlocality of the DPP discussed below.

The focus of this article is on $V_{\rm DPP}(r)$, which depends on the specific characteristics (collectivity, the nature of the strongly coupled channels, etc.) of the interacting nuclei, the energy (particularly in the threshold region) and the effects of the nuclear density gradients that are not represented in a local density model. Local density models cannot lead to L dependence which is predicted by the Feshbach approach and for which there is phenomenological support. The formal expression for $V_{\rm DPP}(r)$, see below, reveals that it is nonlocal and L dependent and hence more properly written $V^L_{\rm DPP}(r, r')$. After many years of optical model studies, the nonlocality and L dependence of $V_{\rm DPP}$ are far from well understood. The physical processes, see subsection III C, that lead to the L dependence and nonlocality are responsible for the fact that the optical model potential cannot be fully represented by a folding model that is based on a local density model. These processes must be understood before nucleon-nucleus or nucleus-nucleus scattering can be said to be understood.

A. Overview of the Feshbach theory

We outline implications of Feshbach's theory of nuclear reactions in order to facilitate the ensuing discussion. The theory provides a formal expression for the entire optical model potential (OMP), but it also provides the basis for a calculation of the contribution of specific coupled channels against a background of many channels that are included phenomenologically. This is justified formally in Ref. [20] and provides a means of calculating the variation in the OMP as nuclear properties change with energy or with Z and A. It also makes it possible to study the contribution of specific coupled channels.

Various calculations of the entire potential have been made, see, for example, Refs. [3,21,22]. Reference [22] includes references to other DPP studies and has a substantial discussion of the nonlocality generated by channel coupling. For simplicity, the present account is for nucleon-nucleus scattering but can be generalized to composite projectiles.

Feshbach defined projection operators P for the target nucleus ground state and Q for the excited states of the target nucleus. They obey the standard rules for projection operators: $P^2 = P$, $Q^2 = Q$, $PQ = QP = 0$, $P + Q = 1$. Formal expressions can be written for the contributions from specific channels by dividing the Q space by writing $Q = p + q$ where p projects onto specific states to be considered, and q projects onto the rest. The q space represents the very many states whose contribution may be considered to vary slowly with N, Z, and E. The difference between the effective potential for the space defined by projection operator $\pi = P + p$ and the effective interaction for space P may be considered to be the DPP that is due to the states included within the space defined by p. The formal justification is

given in Ref. [20], leading to an explicit expression for the DPP, $V_{\rm DPP}$, that requires an evaluation of the complex and nonlocal propagator in terms of Green's functions. It is, in terms of the local coupling potential V_{1m} between the elastic channel (channel 1) and all inelastic channels m within the space defined by p:

$$V_{\rm DPP} = \sum_{m,m' \in p} V_{1m}(r) G_{mm'}(r, r') V_{m'1}(r'). \qquad (2)$$

Being both nonlocal and L dependent, $V_{\rm DPP}$ strictly should be written $V^L_{\rm DPP}(r, r')$. It is important that the interactions V_{1m} and V_{m1} are effective interactions resulting from coupling to the entire q space, although in practice, local representations must be used. Models of the entire OMP, Refs. [3,21,22], effectively consider $p = Q$ with $q = 0$. Equation (2) presumes no coupling to rearrangement channels, pointing to the problem of nonorthogonality when reaction channels are considered.

The Green's function $G_{mm'}(r, r')$ is the coordinate space representation of $1/(E - H)$ and, as such, involves the interchannel coupling between all the channels $m \in p$. Omitting this interchannel coupling is equivalent to replacing propagator G by $G^0 = 1/(E - H_0)$ where H_0 involves a diagonal potential only. In this case, and only in this case, the nonlocal contributions of particular channels are additive, a point that will be important later. An alternative to evaluating Eq. (2) involves carrying out coupled-channels calculations as described in subsection III B.

III. EVALUATION OF THE DPP

Two general methods have been applied to the calculation of $V_{\rm DPP}$: direct evaluation of the Green's function expression, Eq. (2), and "coupled-channels plus inversion," both to be described below. References to earlier work will be found in Ref. [22].

A. Direct evaluation

If coupling between the nonelastic channels is neglected, the Feshbach expression can be directly evaluated as a sum over Green's functions sandwiched between interactions coupling to the elastic channel. For special cases, such as the long-range term generated by Coulomb excitation, analytical evaluation is possible, see, e.g., Refs. [23–25]. More generally, the absence of the analytic properties of the Coulomb interaction and the coupling between the nonelastic channels seriously complicate the evaluation. Advantages of direct evaluation include:

(i) The (nonlocal and L dependent) contribution to the complex potential due to the coupled channels is calculated directly.
(ii) When interchannel coupling is not included, the contributions from different excited states may be directly added.
(iii) The use of the Sturmian [22] method allows a restricted class of interchannel coupling to be included.

Disadvantages or problems with this method:

(i) The L dependence and nonlocality of the resulting potential make it hard to relate to local empirical potentials.
(ii) It is not straightforward to include coupling between the various channels that are coupled to the elastic channel, an elaborate iterative procedure being required except in the cases where the Sturmian method [22] is applicable.
(iii) It is not straightforward to include nonorthogonality and finite-range effects where there is coupling to rearrangement channels. Coulter and Satchler [3] exploit the fact that a zero-range approximation gives separable nonlocal pickup terms.
(iv) The representation of effects arising from antisymmetrization is very difficult.
(v) Angular distributions to specific coupled channels (sometimes important, not least as a check on the calculations) are not a straightforward by-product.

B. Methods based on CC calculations

Early attempts at evaluating the DPP typically involved first performing coupled-channels calculations and then attempting to refit the resulting elastic channel angular distributions with an optical model search code, e.g., Ref. [20]. Subtracting the bare potential of the CC calculation from the result of the potential search gives a measure of the effect of the particular coupled channels but is unsatisfactory because of the ambiguities and the restricted parametrization. A better procedure is to invert the elastic channel S matrix from the CC calculation to obtain an exact local and L-independent representation of the DPP corresponding to the particular channels included in the CC calculation.

Coupled-channels calculations permit any number of channels, collective, breakup, or transfer, to be included, limited only by the available computing power. Finite-range and nonorthogonality corrections are now routinely implemented in transfer calculations. There is no problem with coupling between nonelastic channels. Alternative representations of the DPP can be derived from the elastic channel S matrix, S_{lj}, or the elastic channel stationary state wave function, $\psi_{lj}(\mathbf{r})$, from the CC calculation. We list the main methods:

(i) Efficient $S_l \rightarrow V(r)$ inversion procedures permit a direct evaluation of a local L independent potential that exactly represents the effects of the channel coupling. It is possible to invert S_{lj} for spin-half and $S^j_{ll'}$ for spin-1 projectiles, leading to spin-orbit and T_R tensor interactions.
(ii) Potentials that are spatially dependent (dependent on angle as well as radius) but L independent can be derived directly from the elastic channel wave function [26,27].
(iii) L-dependent trivially equivalent local potentials (TELPs) following the formulation of Franey and Ellis [28].
(iv) The method closest to the exact inversion method is the weighted TELP method as embodied, for example,

in the code FRESCO [6]. It too yields a local and L-independent potential that in certain cases is quite close to that from direct inversion of the S matrix.

Advantages of the CC-plus-inversion method:

(i) Existing CC codes permit large numbers of channels to be included, with full inter-partition coupling incorporating nonorthogonality corrections and finite-range coupling.
(ii) The calculation directly produces the differential cross sections for all coupled channels. This permits comparison with experimental data, thus enabling an evaluation of the whole reaction formalism and the extraction of spectroscopic information.
(iii) For certain strongly coupled inelastic channels [29,30], exchange effects can be included by extending to coupled integrodifferential channels.

Concerning point (iii), the future development of coupled integrodifferential codes would be a key step in nuclear reaction analysis, with inversion providing an exact L-independent representation that can be compared with purely phenomenological potentials. This is useful because model-independent fitting provides potentials giving precise and complete fits to experimental elastic scattering data.

Iterative perturbative (IP) $S_L \rightarrow V(r)$ inversion [7] provides an efficient means for determining the potential corresponding to any theory that determines the S matrix directly, such as theories based on the impulse approximation or the resonating group model. It efficiently determines the local equivalent for any nonlocal potential [31]. All the DPPs presented here are derived using the CC-plus-inversion approach in which IP inversion is applied to the elastic channel S_{LJ} from CC calculations using the code FRESCO [6].

C. Problematic features of the Feshbach approach

By whatever means the DPP is evaluated, there remains a fundamental problem with the Feshbach theory as it is generally applied. The folding model term cannot be calculated with the bare NN interaction, yet the modifications to the interaction to make a folding model tractable clearly involve excitations that are not orthogonal to inelastic excitations. The first, "folding model" term $V_{\rm FM}$ would therefore, in principle, be complex. This is specifically true with folding models derived from elaborate G-matrix calculations [32,33] based on realistic nucleon-nucleon interactions. Current folding models generally involve some form of local density approximation and cannot represent L-dependent effects since they do not contain any representation of the angle between the local nucleon momentum and the gradient of the nuclear density, i.e., a $\mathbf{k}\cdot\mathbf{r}$ term. Particles in reaction channels which do sense the whole nuclear surface would, in general, make L-dependent contributions to the effective potentials in other partitions. The nonorthogonality between particular reaction channels and channels that are implicitly included in G-matrix-derived V_{1m} and V_{m1} suggests the development of an approach that is analogous to the Strutinsky model of nuclear structure. The folding model would provide a smoothly varying background to which fluctuations extracted from the analysis of reaction channel contributions would be added.

With the exact Green's function methods, the treatment of nonorthogonality corrections, and also finite-range corrections to reaction channel contributions, are very difficult. Such problems are less intractable within the CC-plus-inversion procedure. The inclusion of exchange terms is also difficult within the formal Feshbach framework but, as noted above, they could be included in inelastic-scattering calculations within the CC-plus-inversion approach, extended to integrodifferential equations.

IV. COUPLED-CHANNELS CALCULATIONS FOR $p + {}^8$He

We present details of a series of CC calculations involving protons incident on ^{8}He in which the following reaction channels were included: (p,t) to ^{6}He and (p,d) to ^{7}He, including breakup and reorientation channels in the deuteron partition. Full complex remnant terms and nonorthogonality corrections were included in all couplings between partitions.

We determined DPPs for the case when all possible couplings between reaction channels (with some exceptions as noted) were included. However, in order to get a more complete understanding of the contribution of CC channels to elastic scattering, we also carried out calculations with various combinations of reaction channels. In Fig. 1 we show the

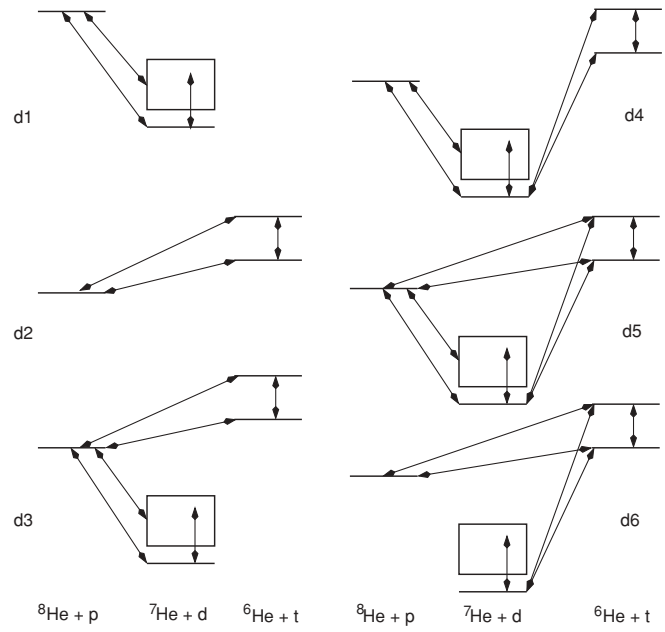

FIG. 1. Schematic representations of the six sets of coupled reaction channels for which results are presented. The case labeled d1 represents pickup to the ^{7}He resonance channel, together with deuteron breakup states of the outgoing deuteron. Case d2 represents direct pickup of a neutron pair leading to ground and 2^+ states of ^{6}He, case d5 represents the "complete" calculation, and d3, d4, and d6 represent the other possible couplings considered. There is no coupling between the deuteron continuum and the triton channels. The text specifies the spins, parities, and energies of the included states.

various possibilities, labeled d1, d2 . . . d6. We shall use these labels extensively throughout this article as we discuss the way in which these processes contribute to the effective $p + {}^8\mathrm{He}$ interaction. We shall also introduce labels for certain modified forms of these cases.

Analyses of cases d1 and d2 show how single-neutron and two-neutron pickup respectively contribute to the nucleon interaction (this seems to be the first evaluation of d2 contributions). Analysis of d3, in which single-neutron and neutron-pair pickup channels are not mutually coupled, will provide information concerning the nonlocality of the pickup DPPs, and the energy dependence of nonlocal effects. Cases d4 and d6 will demonstrate that the "b" channels in the generic "gs <=> a <=> b" coupling can have a major effect on "gs <=> a" coupling. Case d5 is the complete calculation. The parameters for the proton interaction with ^{8}He, as well as the various other parameters, were chosen to give an optimum fit to the elastic scattering and to the (p, d) and (p, t) pickup angular distributions, where available, for the complete calculation designated d5 in Fig. 1. The parameters were then kept fixed for the other coupling systems d1–d4 and d6. The DPPs will be presented for cases d1 to d5 at all energies and for d6 at 15.66 MeV/nucleon. The effects of coupling between the different partitions will become apparent, but the DPP for case d1, for example, will not be exactly what it would be if the parameters had been optimized for that case. We now present the details of the parameters, the channels included and the relevant fits to the elastic channels for case d5.

A. Parameters and fits at 15.66 MeV/nucleon

For protons interacting with ^{8}He at 15.66 MeV/nucleon, elastic scattering was calculated with a renormalized JLM [32] folding model potential together with coupling to $d + {}^7\mathrm{He}$ channels and $t + {}^6\mathrm{He}$ channels according to the schemes labeled d1 to d6 in Fig. 1. The renormalization of the JLM potential was chosen to give the optimum fit to the elastic scattering for case d5, together with acceptable fits to the transfer channel angular distributions. The fact that the renormalization required was a factor of 1.02 for the real part and 0.22 for the imaginary part suggests that in this case the DPP will be predominantly absorptive. That is to say, the channels shown in Fig. 1 are, in this case, evidently the predominant source of absorption from the elastic channel when protons interact with ^{8}He. The fit to the elastic-scattering angular distribution for the complete, d5, calculation is given in Fig. 2 together with the neutron pickup calculation, d1. Figure 3 shows the elastic scattering with no coupling (the bare potential) and cases d1, d2, and d3. It can be seen that the (p, t) effect is, as expected, much smaller than the (p, d) effect, though the effect of the two together, without direct coupling between the d and t channels (i.e., case d3) is much greater than d1 alone near the minimum at 65°. However, comparison with the previous figure shows that the coupling between the d and t partitions makes a crucial contribution to the fit at this minimum.

The full calculation, case d5, was as described in Keeley *et al.* [12]; we specify it here for ease of reference. The entrance channel JLM potential was calculated using the no-core shell model ^{8}He density of Navrátil and Barrett [34]. In the $d + {}^7\mathrm{He}$ exit channel the CDCC formalism was employed to model the effects of deuteron breakup, with potentials of Watanabe single-folding type using n and p plus ^{7}He optical potentials calculated according to the global parametrization of Koning and Delaroche [35]. These were adjusted to give the best fit to the measured (p, d) angular distribution, an increase of a factor of 2 in the depth of the imaginary potential wells being necessary to give a good description of the data at angles greater than 50° in the center-of-mass frame. Couplings to deuteron breakup states with the neutron and proton in relative S and D states were included, along with all allowed continuum-continuum couplings up to multipolarity $\lambda = 2$. The neutron pickup transfer step was calculated using the Reid soft-core potential [36] to bind the neutron and

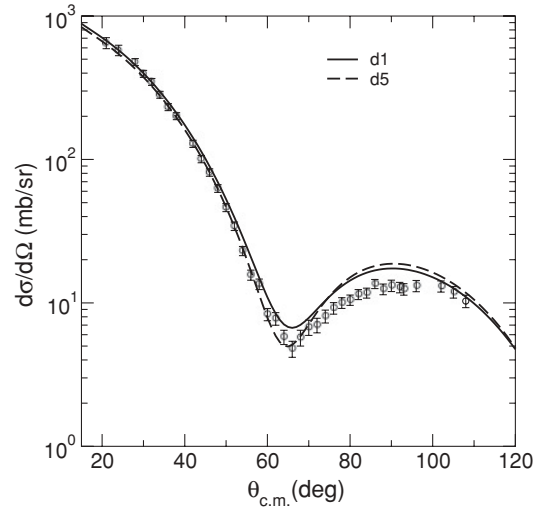

FIG. 2. For proton elastic scattering from ^{8}He at 15.66 MeV/nucleon, the calculated fit to the data for the full (d5) calculation and the d1 case (neutron pickup).

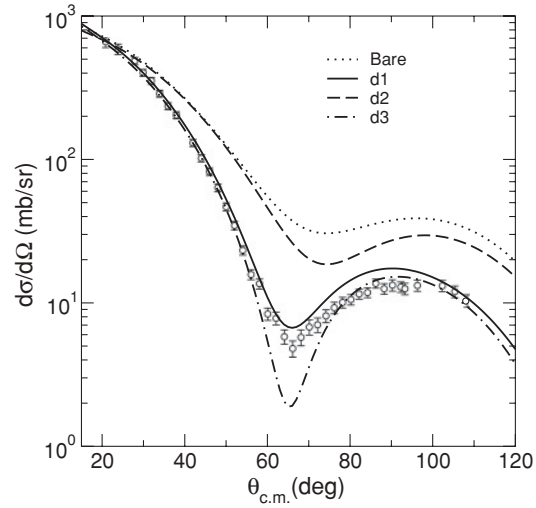

FIG. 3. For proton elastic scattering from ^{8}He at 15.66 MeV/nucleon, the calculated fit to the data with the bare potential (no coupling) and for the CC cases d1, d2, and d3.

proton, including the small D-state component of the deuteron ground state; the same interaction was used to calculate the exit channel deuteron potentials. The $n + {}^7$He binding potential was of standard Woods-Saxon form, with radius $R_0 = 1.25 \times 7^{1/3}$ fm, $a_0 = 0.65$ fm, the well depth being adjusted to give the correct binding energy. Pickup to unbound states of the "deuteron" was included in addition to transfer to the ground state.

The potential in the $t + {}^6$He exit channel was based on the ${}^3\text{He} + {}^6\text{Li}$ parameter set A of Basak *et al.* [37], as no suitable triton potentials are available. The ^{6}He $0_1^+ \rightarrow 2_1^+$ coupling was included using a standard collective model form factor and the isoscalar deformation length of Khoa and von Oertzen [38], the potential parameters being adjusted to recover the same $t + {}^6$He elastic scattering given by an optical model calculation using the unaltered parameters of Ref. [37]. The adjusted potential parameters are given in Table 1 of Ref. [12]. Direct stripping of the two neutrons to both the 0_1^+ ground and 1.8 MeV 2_1^+ excited states in ^{6}He assumed transfer of a di-neutron-like cluster. The ${}^2n + p$ binding potential was taken from Guazzoni *et al.* [39] and the ${}^2n + {}^6$He potential was of Woods-Saxon form with radius $R_0 = 2.5$ fm, close to the matter radius of ^{8}He, and diffuseness 0.7 fm.

The ${}^8\text{He}(p, d){}^7\text{He}(d, t){}^6\text{He}$ two-step transfer was included in addition to direct pickup of the two neutrons. The $n + d$ binding potential was taken from Eiró and Thompson [40] and the $n + {}^6$He potential was of Woods-Saxon form with parameters $R_0 = 1.25 \times 6^{1/3}$ fm, $a_0 = 0.65$ fm. The ${}^7\text{He}/{}^6\text{He}_{0+}$ form factor was calculated within a bin of width 320 keV with the potential depth adjusted to give a resonance at the correct energy: doubling the width of the bin did not change the results of the calculation.

The various spectroscopic amplitudes required are listed in Ref. [12], those for the light particle overlaps being fixed from the literature, as were those for the $n + {}^6$He overlaps, the rest being obtained by fitting the ensemble of the available data, as described in Ref. [12].

B. Parameters and fits at 25 MeV/nucleon

The calculations at 25 MeV/nucleon were exactly as described above for 15.66 MeV/nucleon, with the exception of the optical potentials in the entrance and exit channels. The entrance channel JLM potential was calculated with the same ^{8}He density but for the appropriate incident energy. The Watanabe single-folding potentials in the $d + {}^7$He exit channel were calculated using the global parametrization of Koning and Delaroche for the n and $p + {}^7$He potentials. No adjustment of these potentials was made in this case. Finally, the $t + {}^6$He potential in the exit channel was derived from the ${}^3\text{He} + {}^6\text{Li}$ set B potential of Görgen *et al.* [41], the parameters being adjusted to recover the same $t + {}^6$He elastic scattering from a CC calculation, including the ^{6}He $0_1^+ \rightarrow 2_1^+$ coupling as given by an optical model calculation using the unaltered potential of Ref. [41]. The resulting parameters are given in Table I.

To fit the elastic-scattering data [42] at 25 MeV/nucleon with the full, d5, calculation, quite extreme measures were required: the JLM real part was multiplied by a factor of 0.85 and the imaginary part was multiplied by 0.05. This implies that almost all the absorption for this case is a result of reaction channel coupling; in subsection VI B, we describe steps taken to determine the extent that the extracted DPP depends on the extreme normalization of the imaginary part. The d5 calculation fit to the measured elastic-scattering differential cross section is shown as a solid line in the upper panel of Fig. 4. The dashed line presents the calculation with the same renormalized JLM potential ("bare" potential) but with coupling switched off. The lower panel shows the effect of the coupling on the analyzing power, for which there are no measurements in this energy range.

TABLE I. The $t + {}^6$He potential parameters for the 25 MeV/nucleon calculation. The real part is of Woods-Saxon and the imaginary part of Woods-Saxon derivative form.

V	r_V	a_V	W_D	r_D	a_D
70.0	1.35	0.75	5.74	1.61	0.9

C. Parameters and fits at 61.3 MeV/nucleon

The calculations at 61.3 MeV/nucleon were also as described for 15.66 and 25 MeV/nucleon, with the exception of the optical potentials in the entrance and exit channels. The entrance channel JLM potential was calculated with the same ^{8}He density but for the appropriate incident energy. As there are no elastic-scattering data available at an incident energy of 61.3 MeV/nucleon the normalization factors of the JLM potential in the d5 calculation were adjusted to match an optical model calculation using the JLM potential with both real and imaginary parts renormalized by factors of 0.8. This prescription was found to give a reasonable description

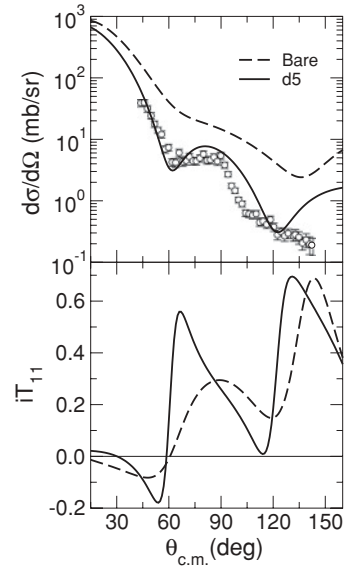

FIG. 4. For proton elastic scattering from ^{8}He at 25 MeV/nucleon, the solid line shows the calculated fit to the data for the full, d5, calculation. The dashed line is with the d5 couplings all switched off. The upper panel shows the differential cross section, the lower panel the analyzing power.

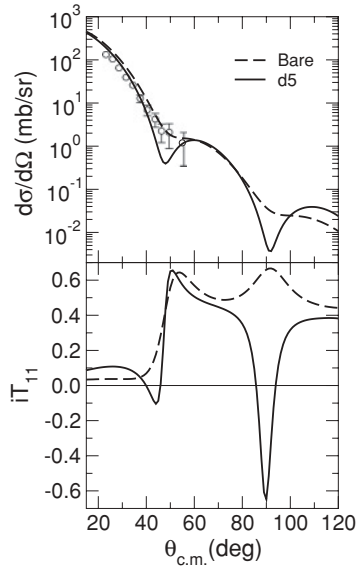

FIG. 5. For proton elastic scattering from ^{8}He at 61.3 MeV/nucleon, the upper panel compares the angular distribution for the full, d5, calculation (solid line) with that (dashed line) when all the couplings are turned off. The circles denote the 66 MeV/nucleon data of Ref. [43]. The lower panel compares the analyzing powers for the same two cases.

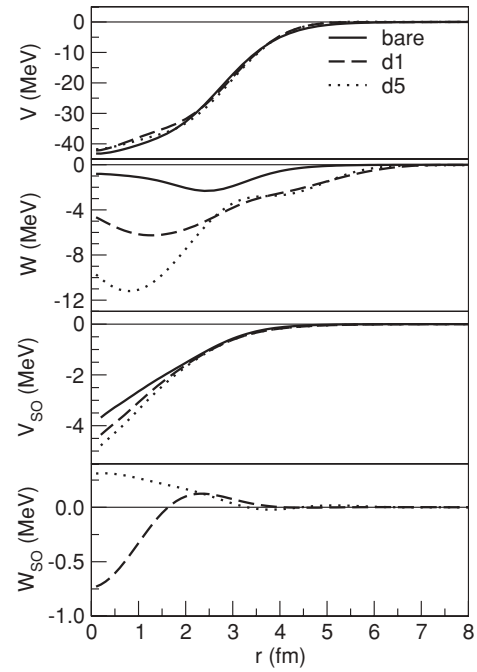

FIG. 6. For 15.66 MeV/nucleon protons, the bare potential and the inverted potential for case d1 and the full calculation, d5. As in subsequent figures, the potentials are ordered as follows from the top down: real central, imaginary central, real spin-orbit, and imaginary spin-orbit.

of the existing $^8\mathrm{He} + p$ elastic-scattering data in this energy region. A limited data set is available for the nearby incident energy of 66 MeV/nucleon [43] and we compare the bare, no-coupling, and full, d5, calculations with it in Fig. 5. The resulting normalization factors of the JLM potential for the d5 calculation were 0.9 (real) and 0.7 (imaginary), suggesting that, at this energy, the DPP will be found to be repulsive and absorptive but to a more modest extent than at the lower energies. Analyzing power data is expected to become available for this reaction at 71 MeV/nucleon, having recently been measured for ^{6}He projectiles [44]. The effect on the analyzing power seen in the lower panel of Fig. 5 suggests that a search for spin-orbit parameters must be undertaken in the context of d5-type calculations, a substantial project for future work.

The Watanabe single-folding potentials in the $d + {}^7$He exit channel were calculated using the global parametrization of Koning and Delaroche for the n and $p + {}^7$He potentials. No adjustment of these potentials was made in this case. The $t + {}^6$He potential in the exit channel was derived from the 72-MeV type A $^3\mathrm{He} + {}^6$Li potential of Bragin *et al.* [45], the parameters being adjusted to recover the same $t + {}^6$He elastic scattering from a CC calculation, including the ^{6}He $0_1^+ \rightarrow 2_1^+$ coupling as given by an optical model calculation using the unaltered potential of Ref. [45]. The resulting parameters are given in Table 1 of Ref. [12].

V. CALCULATION OF THE DPP

A. The DPP for 15.66 MeV/nucleon protons

As in earlier work, Ref. [10,11] and articles cited therein, we apply $S_{lj} \rightarrow V(r)$ inversion, using the IP method [7,46,47], to the diagonal (elastic-scattering) part of the S matrix produced in the CC calculations to yield a potential $V_{\mathrm{cc}}(r)$. The resulting local potential precisely reproduces in an optical model code the theoretical elastic scattering from the CC calculations. The complex potential $V_{\mathrm{cc}}(r)$ contains a complex spin-orbit term. The difference $V_{\mathrm{DPP}}(r) = V_{\mathrm{cc}}(r) - V_{\mathrm{bare}}(r)$, between $V_{\mathrm{cc}}(r)$ and the bare potential $V_{\mathrm{bare}}(r)$, is a local and L-independent representation of the contribution of the coupled pickup channels to the DPP of the proton-nucleus potential.

Figure 6 compares the bare potential $V_{\mathrm{bare}}(r)$ (solid curve) with the inverted potentials $V_{\mathrm{cc}}(r)$ for cases d1 (dashes) and d5 (dots). The contribution of reaction channel coupling to the imaginary central term is huge, but the contribution to the much larger real central term is not negligible; they are more clearly seen by examining the DPP itself, $V_{\mathrm{DPP}}(r)$, presented for cases d1 and d5 in Fig. 7. There are too many DPPs to be clearly compared in a reasonable number of figures. However, they can usefully be quantified using the conventionally defined [5] real and imaginary volume integrals, J_R and J_I and rms radii, $R_R = (\sqrt{\langle r^2 \rangle})_R$ and $R_I = (\sqrt{\langle r^2 \rangle})_I$. Table II presents characteristics of the bare potential and the various inverted potentials; the volume integrals and rms radii for central components and volume integrals for spin-orbit components.

One significant point is that the coupling has a systematic effect on the rms radius of the real potential, reducing it by some 10%. This reflects the fact, already clear from Fig. 7, that the real central part of the DPP is not proportional, as a function of r, to the corresponding term of the bare potential. This has obvious consequences for any attempt to relate nuclear sizes to the radial extension of the OMP. It shows why it is not

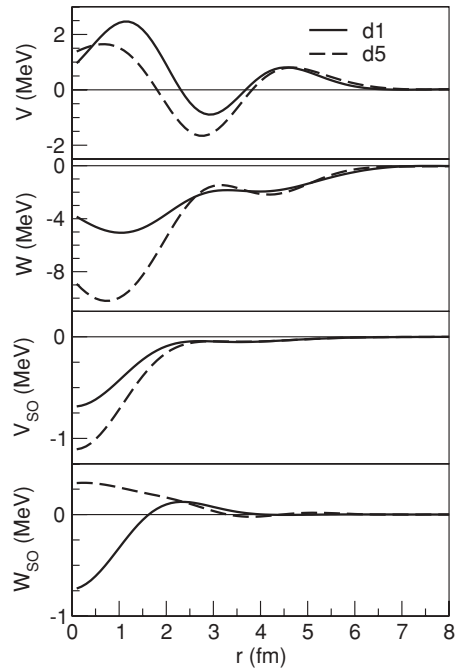

FIG. 7. For 15.66 MeV/nucleon protons, the DPPs for case d1 and the full case, d5.

appropriate to fit data by multiplying folding model potentials with an overall normalization; this can be meaningful only in cases where the fit is sensitive only to a narrow radial range.

The volume integrals of the central components constitute a useful way of characterizing the DPPs, and Table III presents them, calculated by subtracting the corresponding values for the bare potential. Certain results stand out: the DPP for case d1 has a very much larger imaginary term than that for d2, and this relates directly to the much larger deviation of the d1 $d\sigma/d\Omega$ from the "bare" $d\sigma/d\Omega$ in Fig. 3 than for the d2 case. Other points to note:

(i) The DPPs for cases d1 and d2 do not add up exactly to the DPP for case d3. In earlier studies, DPPs for mutually uncoupled channels (here, mutually uncoupled *sets* of coupled channels) have been found to add quite closely to give the total DPP when both channels are coupled to the entrance channel. The present nonadditivity is discussed below in connection with the effects of nonlocality. We note, for comparison with the same ratios at higher energies, that the ratios of the quantities in the d1 + d2 line to the same quantities in the d3 line are not very close to 1.0, being 1.18 for the real part and 0.846 for the imaginary part.

(ii) Coupling of the deuteron channels to the triton channels (case d4) surprisingly reverses the sign of the real DPP due to deuteron channel coupling and similarly reduces the repulsion in the comparison between d3 and d5. This effect is energy dependent, as will be seen.

(iii) Reaction channels have a substantial effect on the spin-orbit potential, generating an imaginary part in all cases except, reassuringly, those involving the pickup of a spin-zero neutron pair, d2 and also d6 to a lesser extent. Although the imaginary spin-orbit DPP for d2 is small, it was necessary to allow its inclusion for a satisfactory inversion.

(iv) Concerning the coupling to the ^{6}He channels, we found: (i) DPPs for the 2^+ state alone are two orders of magnitude smaller than for the 0^+ state alone; (ii) DPPs for the 0^+ alone and the 2^+ alone add very closely to give the DPP when both states are included without coupling between them; coupling between the 2^+ and 0^+ states, as in case d2, increases the imaginary DPP by 10% and reduces the magnitude of (the negative) real DPP by 2%, to give the numbers in row 2 of Table III.

TABLE II. For 15.66 MeV/nucleon, characteristics of the bare potential and the inverted potentials corresponding to coupling schemes d1 to d6. In all tables, volume integrals are expressed in units of MeV fm^3 and rms radii in fm.

Case	Real central		Imag. central		Real S-O	Imag. S-O
	J_R	$R_{\rm rms}$	J_I	$R_{\rm rms}$	$J_{R-\rm SO}$	$J_{I-\rm SO}$
Bare	683.79	3.090	60.84	3.342	25.96	0.0
d1	637.51	2.845	256.53	4.307	30.55	−1.131
d2	606.03	2.900	80.736	3.323	26.37	0.018
d3	578.51	2.571	312.73	4.190	31.67	−2.123
d4	691.76	2.888	284.00	4.248	32.68	−3.553
d5	650.52	2.767	265.05	4.117	31.24	−2.422
d6	592.42	2.869	90.705	3.399	27.08	−0.059

TABLE III. For 15.66 MeV/nucleon, volume integrals of the central components of the DPPs generated by coupling according to schemes d1 to d6. The row "d1 + d2" presents the sum of the DPPs for d1 and d2 couplings.

Case	Real central	Imag. central
	J_R	J_I
d1	−46.28	195.69
d2	−77.76	19.90
d3	−105.28	251.89
d4	7.97	223.16
d5	−33.27	204.21
d6	−91.37	29.864
d1 + d2	−124.04	215.59

B. The DPP for 25 MeV/nucleon protons

Table IV presents characteristics of the bare potential and the various inverted potentials for 25 MeV/nucleon. The volume integrals are not the full story, and the DPPs presented in Fig. 8 show that at 25 MeV/nucleon the full, d5, calculation is roughly approximated by the d3 calculation, in which there is no mutual coupling between the deuteron and triton partitions. The repulsion for case d5 has a peak at the nuclear center, but there is also an extended repulsive region further out, with the net effect of reducing the rms radius of the real central term by about 0.45 fm, about 15%.

TABLE IV. For 25 MeV/nucleon, characteristics of the bare potential and the inverted potentials corresponding to coupling schemes d1, d2, d3, d4, and d5.

Case	Real central		Imag. central		Real S-O	Imag. S-O
	J_R	$R_{\rm rms}$	J_I	$R_{\rm rms}$	$J_{R-{\rm SO}}$	$J_{I-{\rm SO}}$
Bare	523.33	3.090	14.88	3.373	26.47	0.0
d1	440.18	2.697	218.90	4.049	30.58	−0.533
d2	463.27	2.931	27.183	3.260	26.89	0.251
d3	399.88	2.444	267.04	3.942	31.75	−1.799
d4	489.23	2.735	258.20	3.904	32.76	−3.939
d5	462.36	2.641	243.53	3.856	32.39	−2.338

The bare potential found by fitting the elastic scattering at this energy, in a full, d5, calculation, was very different from that found at 15.66 MeV/nucleon, the imaginary component being a factor of 4 less. This may in part be a result of the quality of data that were fitted. In subsection VI A we exploit this case to discuss how the extracted DPPs depend on the bare potential.

Table V presents the volume integrals of the DPPs for the central components by subtraction of the bare potential of row 1 in Table IV. We see that the d3 DPPs are slightly closer to the sum of the d1 and d2 contributions than for 15.66 MeV/nucleon. The ratios of the quantities in the d1 + d2 and the d3 lines are 1.16 for the real part and 0.927 for the imaginary part.

The overall pattern of the DPPs at 25 MeV/nucleon is consistent with what was found for 15.66 MeV/nucleon except that in case d4, although coupling to the triton channel still reduces the repulsive effect of case d1, the effect at

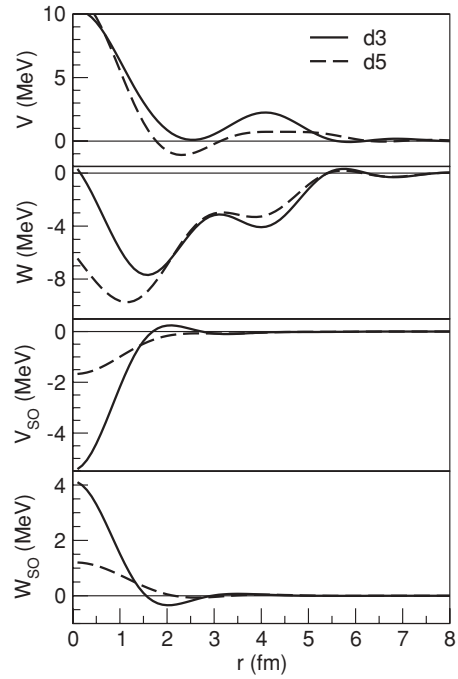

FIG. 8. For 25 MeV/nucleon protons, the DPPs for case d3 and the full case, d5.

TABLE V. For 25 MeV/nucleon, volume integrals of the central components of the DPPs generated by coupling according to schemes d1, d2, d3, d4 and d5. The row "d1 + d2" presents the sum of the DPPs for d1 and d2 couplings. The bare potential that is subtracted in these cases is given in the top row of Table IV.

Case	Real central	Imag. central
	J_R	J_I
d1	−83.15	204.02
d2	−60.06	27.18
d3	−123.45	252.16
d4	−34.10	243.32
d5	−60.97	228.65
d1 + d2	−143.21	231.2

25 MeV/nucleon is much less marked and does not reverse the sign of the real part of the DPP. The d4 DPP is, like the d1 DPP, repulsive. The effect on the spin-orbit potential of the neutron pair transfer is again small at this energy.

C. The DPP for 61.3 MeV/nucleon protons

Table VI presents characteristics of the bare potential and the various inverted potentials for 61.3 MeV/nucleon. The bare potential has a shallower real central term and a much deeper imaginary central term than for 25 MeV/nucleon. The DPPs presented in Fig. 9 show that at this higher energy, the full, d5, calculation is quite closely approximated by the d3 calculation, in which there is no mutual coupling between the deuteron and triton partitions. The repulsion has a peak at the nuclear center but also has an extended region further out with the net effect of reducing the rms radius of the real central term by about 0.3 fm, about 10%. The qualitative features are the same as at 25 MeV, but the wavy features have a shorter wavelength, as expected.

Table VII presents volume integrals characterizing the DPPs for the central parts, calculated by subtraction of the bare potential. A number of trends become more definite at 61.3 MeV/nucleon. The DPPs for case d2 are now very much smaller in magnitude than those for case d1. This is a significant energy dependence: recall that at 15.66 MeV/nucleon, the

TABLE VI. For 61.3 MeV/nucleon, characteristics of the bare potential and the inverted potentials corresponding to coupling schemes d1, d2, d3, d4, and d5. The double occurrence of 283.57 in column 4 is coincidental and not a misprint.

Case	Real central		Imag. central		Real S-O	Imag. S-O
	J_R	$R_{\rm rms}$	J_I	$R_{\rm rms}$	$J_{R-{\rm SO}}$	$J_{I-{\rm SO}}$
Bare	389.46	2.981	158.65	3.224	23.57	0.0
d1	342.50	2.719	277.28	3.387	24.56	−2.310
d2	374.88	2.950	162.91	3.213	23.75	−0.066
d3	330.26	2.660	283.57	3.379	22.35	−1.704
d4	341.11	2.712	284.56	3.386	23.09	−1.305
d5	335.81	2.688	283.57	3.377	22.89	−1.505

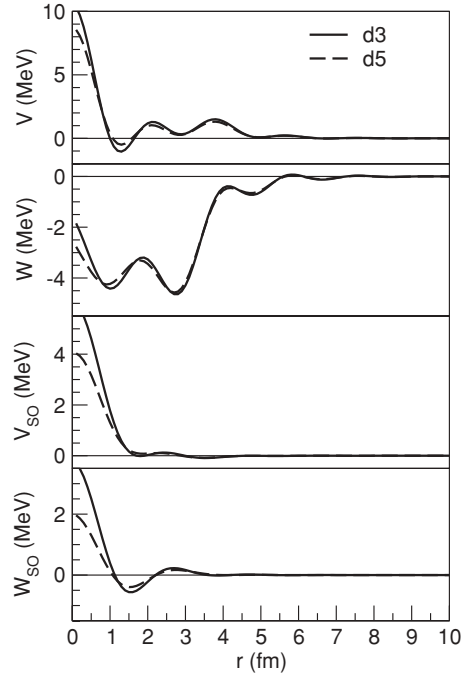

FIG. 9. For 61.3 MeV/nucleon protons, the DPPs for cases d3 and the full case, d5.

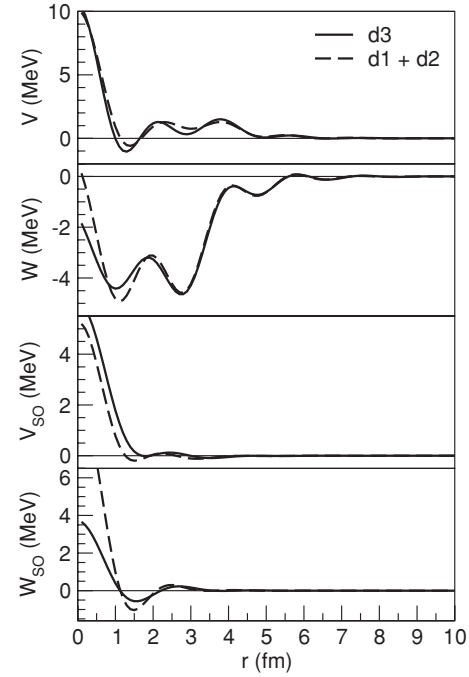

FIG. 10. For 61.3 MeV/nucleon protons, comparing the DPP for case d3 (solid line) with the sum of the DPPs for cases d1 and d2 (dashes).

repulsive real DPP for case d2 was larger in magnitude than it was for d1. At 25 MeV/nucleon the d2 repulsion was smaller than for d1. The repulsion due to neutron pickup, d1, remains substantial at 61.3 MeV/nucleon, especially as a fraction of the bare potential. The effect on the spin-orbit potential of neutron pair transfer is again very small.

It is clear from the 25 and 61.3 MeV/nucleon cases that the additivity of DPPs due to mutually uncoupled partitions holds more closely at higher energy, as can be seen by comparing the d1 + d2 DPPs with the d3 DPPs at all three energies. At 61.3 MeV/nucleon, the ratios for the real and imaginary terms are 1.04 and 0.984, respectively, much closer to unity than the values at 15.66 and 25 MeV/nucleon. The additivity is also close point by point at 61.3 MeV, as can be seen in Fig. 10.

TABLE VII. For 61.3 MeV/nucleon, volume integrals of the central components of the DPPs generated by coupling according to schemes d1, d2, d3, d4, and d5. The row "d1 + d2" presents the sum of the DPPs for d1 and d2 couplings. The bare potential that is subtracted is given in the top row of Table VI.

Case	Real central	Imag. central
	J_R	J_I
d1	−46.96	118.63
d2	−14.58	4.26
d3	−59.20	124.92
d4	−48.35	125.91
d5	−53.65	124.92
d1 + d2	−61.54	122.89

The tendency for $|J_R|$ of the full, d5, DPP to be smaller in magnitude than for case d3, decreases with energy. The difference, substantial at 15.66 MeV/nucleon and intermediate at 25 MeV/nucleon, has almost disappeared at 61.3 MeV/nucleon.

Case d4 also exhibits a significant trend: at the lower energies, the coupling to the triton channels reduced the repulsive effect of the neutron pickup (d1 case), actually reversing the sign at 15.66 MeV/nucleon. At 61.3 MeV/nucleon, the real d4 DPP is actually slightly greater in magnitude than the real d1 DPP, i.e., the repulsive effect has increased. That is to say, the effect of coupling the triton reaction channel has changed with energy in a significant qualitative manner.

The different energy dependencies of the d1 and d2 cases is probably due to variation with energy of the degree of angular-momentum mismatching. In particular, the mismatch for ground-state (p, t) transfer rises from $-2.9\hbar$ at 15.66 MeV/nucleon to $-4.4\hbar$ at 61.3 MeV/nucleon. For the (p, d) vertex these values are just $-1.1\hbar$ and $-2.4\hbar$. This change, together with the greater absorption of tritons, suggests why the d2 DPP falls much more rapidly with energy than the d1 DPP.

VI. DEPENDENCE OF THE DPP ON CALCULATION PARAMETERS

We now discuss the extent to which the calculated DPPs are independent of various parameters. The DPPs presented above were determined for calculations in which the optical model parameters had been optimized to suit the d5 case. In principle, for all CC calculations, the potentials for a specific partition

should be readjusted according to what other partitions or channels are coupled to that partition. To do this consistently for all calculations is out of the question for practical reasons. It is therefore important to know how the DPPs depend on the particular choices of bare potentials; the observables and the actual inverted potentials will certainly depend on them. Here we address the stability of key results against changes of optical model parameters. For the 15.66-MeV/nucleon case, we also study the importance of a correct treatment of the deuteron continuum. Finally, we also investigate the sensitivity of our key results to a change in sign of the ^{6}He $+ 2n$ spectroscopic amplitude.

A. Parameter dependence for 15.66 MeV/nucleon protons

As indicated in Fig. 1, case d1 calculations and all the others involving $d + ^7$He channels, include coupling to the deuteron continuum, calculated using CDCC. In order to determine whether deuteron breakup makes an essential contribution to the DPP, a number of variants of the d1 and d5 calculations have been carried out. These correspond to the lines labeled d5NC, d1NC, d1NCNR, and d1A in Table VIII and Table IX. Cases d1NC and d5NC are variants of cases d1 and d5 in which the continuum states in deuteron channels are omitted but in which the deuteron reorientation is retained. In case d1NCNR, reorientation is also omitted. We did not succeed in performing FRESCO calculations with breakup represented by the continuum but no reorientation. Case d1A involved the adiabatic approximation treatment of deuteron breakup.

Table VIII and Table IX also include cases (d2t, d3t, d4t) in which the imaginary potential in the triton partition was halved. This was done to determine the dependence of the effective proton elastic potential on the nature of the potential in a coupled partition, in this case the $t + ^6$He partition.

Comparing Table IX with Table III, the d1NC and d5NC cases show that the explicit inclusion of the deuteron continuum is essential. Its omission leads to an overestimation of the pickup contribution to the real part of the central DPP and an underestimation of the imaginary part. Comparing Table VIII and Table II, we find that the deuteron continuum also changes the sign of the induced imaginary spin-orbit potential although, surprisingly, reorientation had little effect, case d1NCNR. The d1A case suggests that representing deuteron breakup with the adiabatic model is not adequate for these purposes, the DPP being very like that found with no coupling to the continuum. In summary, deuteron breakup makes an important contribution to the absorption in the proton channels and simultaneously moderates the induced repulsion.

A substantial reduction in the absorption in the triton channels (compare cases d2 with d2t, etc.) leads to a very small reduction of the absorption in the proton channel, as measured by the reduction in the imaginary parts of the DPPs. Nevertheless, the small decrease in the imaginary DPP when the triton imaginary potential is reduced suggests that the triton partition acts as a doorway for absorption of protons.

TABLE VIII. For 15.66 MeV/nucleon, characteristics of the bare potential and the inverted potentials corresponding to modified treatment of the deuteron breakup; refer to the text for an explanation of NC, NCNR and A. The results for cases d2 to d4 with the imaginary potential in the triton partition halved, are labeled d2t, d3t, and d4t.

Case	Real central		Imag. central		Real S-O	Imag. S-O
	J_R	$R_{\rm rms}$	J_I	$R_{\rm rms}$	$J_{R-{\rm SO}}$	$J_{I-{\rm SO}}$
Bare	683.79	3.090	60.84	3.342	25.96	0.0
d1NC	609.48	2.713	198.60	4.138	30.090	1.050
d1NCNR	612.05	2.716	197.90	4.134	29.461	0.786
d1A	604.35	2.762	195.69	4.283	27.99	−2.162
d5NC	621.63	2.627	197.62	3.984	32.409	1.534
d2t	601.95	2.900	75.952	3.336	26.37	0.016
d3t	572.12	2.565	311.50	4.189	31.85	−2.065
d4t	700.18	2.880	281.81	4.239	33.463	−2.571

TABLE IX. For 15.66 MeV/nucleon, volume integrals of the central components of the DPPs corresponding to cases in Table VIII.

Case	Real central	Imag. central
	J_R	J_I
d1NC	−74.31	137.76
d1NCNR	−71.74	137.06
d1A	−79.44	134.85
d5NC	−62.16	137.78
d2t	−81.84	15.11
d3t	−111.67	250.66
d4t	16.39	220.97

B. Parameter dependence for 25 MeV/nucleon protons

We studied the dependence of the DPPs on substantial changes in the bare nucleon potential. Cases d1 to d5 were repeated using the very different bare proton potential that had been used at 15.66 MeV/nucleon. The inverted potentials in Table X and the DPPs in Table XI are labeled d1x to d5x.

The overall pattern of the DPPs is the same for the two bare potentials. The repulsion for triton coupling is less than that for deuteron coupling (compare d2x and d1x) as was seen in

TABLE X. For 25 MeV/nucleon, characteristics of the 15.66 MeV/nucleon bare potential and the inverted potentials, labeled d1x, d2x, d3x, d4x and d5x, calculated with the 15.66 MeV/nucleon bare potential of row 1.

Case	Real central		Imag. central		Real S-O	Imag. S-O
	J_R	$R_{\rm rms}$	J_I	$R_{\rm rms}$	$J_{R-{\rm SO}}$	$J_{I-{\rm SO}}$
Bare	683.79	3.090	60.84	3.342	25.96	0.0
d1x	617.16	2.858	256.51	3.933	29.98	−0.801
d2x	630.90	3.000	74.595	3.294	26.37	0.289
d3x	580.76	2.725	299.57	3.861	30.48	−0.799
d4x	662.97	2.855	281.30	3.861	31.75	−3.150
d5x	638.15	2.797	267.07	3.812	31.99	−2.297

TABLE XI. For 25 MeV/nucleon, volume integrals of the central components of the DPPs generated when the bare proton potential used for 15.66 MeV/nucleon was applied. The row "d1x + d2x" presents the sum of the d1x and d2x DPPs.

Case	Real central	Imag. central
	J_R	J_I
d1x	−66.30	195.67
d2x	−52.89	13.75
d3x	−103.03	237.38
d4x	−20.82	220.46
d5x	−45.64	206.23
d1x + d2x	−119.19	209.42

Table V, in contrast to the situation at 15.66 Mev/nucleon and consistent with the continuing trend at 61.3 MeV/nucleon, subsection V C. The ratios of the quantities in the d1x + d2x and d3x lines are 1.16 and 0.882 for the real and imaginary parts, respectively. Recall that the corresponding values in the d1 + d2 and the d3 lines of Table V were 1.16 and 0.927 so the considerable difference in the bare potential had no effect on the ratio for the real DPP and very little effect on the imaginary DPP.

We conclude that the general character of the DPPs that we find is robust, as is shown by the findings: (i) DPPs for 25 MeV/nucleon calculated with the potential appropriate to 15.66 MeV/nucleon are very similar to those calculated with the very different potential determined for 25 MeV/nucleon and (ii) substantial changes in the triton potential have quite small effects in cases d2t, d3t, and d4t at 15.66 MeV/nucleon.

C. Dependence on spectroscopic amplitude

We investigated the dependence of our results on the sign of the 2*n* spectroscopic amplitude. This was originally determined in the course of fitting the reaction observables, including the angular distributions of tritons feeding the ^{6}He states [12]. We carried out d5 calculations at 15.66 and 61.3 MeV/nucleon in which the sign of $^7\mathrm{He} + n$ spectroscopic amplitude is reversed. This is equivalent to changing the sign of the 2*n* spectroscopic amplitudes for both states in ^{6}He. At the lower energy the effect on the elastic-scattering angular distribution was considerable and any reasonable modification of the OM parameters is unlikely to fit the data. Nevertheless, all the qualitative features of the DPPs were broadly the same; the volume integrals of the real and imaginary central terms (all in MeV fm^3) were −36.74 and +356.29 compared to the previous values of −33.27 and +204.21. At 61.3 MeV/nucleon, changing the sign made a relatively small difference to the elastic-scattering angular ditributions. The central DPP volume integrals became −59.25 (real) and +141.74 compared to the previous values of −53.65 and +124.92, respectively. In summary, although the fits to the observables [12] strongly support the spectroscopic amplitudes used above, it is the case that a different sign for the 2*n* spectroscopic amplitude would leave our major findings concerning the strong DPPs unaffected.

VII. THE NONLOCALITY OF THE DPP

References to nonlocality in the nuclear physics literature frequently assume that it has the well-known Perey-Buck form, or the Fock term of the nucleon potential, the former essentially a phenomenological representation of the latter. A consideration of the Perey-Buck nucleon potential folded into composite particles leads [19] to the conclusion that for heavy projectiles, the nonlocality is of short range. But explicit DPPs calculated from the Feshbach formalism [3,21,22] are highly nonlocal in a way that differs significantly from the Perey-Buck form. What consequences does this underlying nonlocality of the DPP have for the local equivalents?

Formally, it is clear that DPPs arising from sets of channels that have no mutual coupling add. This holds quite well for local DPPs that are smaller in magnitude than in the present case. (At 15.66 MeV/nucleon and 25 MeV/nucleon, the imaginary part of the DPP far exceeds the imaginary part of the bare potential.) However, strictly, the additivity applies to the underlying nonlocal DPPs and not to the local equivalents. Since we have calculated local DPPs for nonmutually coupled sets of channels at all three energies, the additivity can be tested. The sets of channels corresponding to the d1 and d2 processes are not mutually coupled in the d3 calculations, and in Tables III, V, VII, and XI we have presented in rows labeled "d1 + d2" the sums of the corresponding quantities in rows d1 and d2. The results have been discussed quantitatively for each energy. Figure 10 shows that additivity applies, point by point, at 61.3 MeV/nucleon, but the tabulated volume integrals show that it is only approximate at lower energies. However, even at the lowest energy, weaker DPPs add, as discussed in subsection V A in connection with the coupling to the 0^+ and 2^+ states of ^{6}He.

The general effects of nonlocality have been discussed by Austern [48]. One characteristic feature is that flux is removed from the elastic channel in one region of the target and fed back elsewhere; an explicit example for inelastic scattering is given in Ref. [26]. This idea suggests an interpretation of the fact that, for strongly absorbed particles, channel coupling often results in an *increase* in $|S_L|$ over a range of L values, typically for lower L. For protons however, in all the cases discussed here, coupling decreases $|S_L|$, as expected for processes that absorb flux from the elastic channel.

In the present case, we can infer that nonlocality has had a substantial effect. The fact that the local equivalents of nonlocal potentials do not add exactly can be seen by noting that the semiclassical approximate local equivalents to nonlocal potentials involve the local momentum in the nucleus and must therefore be calculated by an iterative self-consistent method. Since the local momentum depends on the potential, local equivalents of nonlocal potentials cannot add exactly.

As a simple example, the local equivalent of twice the Perey-Buck potential is clearly not twice the local equivalent of the Perey-Buck potential. Perey and Buck's approximate

expression for the relation between the depth V_N of a nonlocal nucleon potential of their form and the depth within the nucleus of V_L the equivalent local potential for nucleons of energy E/MeV is

$$V_N = V_L \exp\left[\frac{\beta^2}{84}(E + V_L)\right]. \quad (3)$$

Clearly, adding two nonlocal potentials does not lead to a local potential that is the sum of the local equivalents; for example, doubling a nonlocal potential does not double the local equivalent potential. To take a concrete case, for 20 MeV nucleons and $\beta = 0.85$, we trivially find that values of V_N of 46, 67, 91.2, and 119.4 MeV correspond respectively to $V_L = 30,\ 40,\ 50,\ 60$ MeV with values of $V_N/V_L = 1.53$, 1.68, 1.82, and 1.99.

Although the exact nature of the nonlocality of the reaction channel DPP is unknown, we have found a plausible explanation for nonadditivity of the local equivalents. The additivity is more exact at the higher energy because, at the higher external energy, the local energy at radius r is less dependent on the (nonlocal) potential around r. Nevertheless, the non-locality of the DPP differs substantially from that arising from exchange, a point stressed by Rawitscher [22]. That author also points out that the "Perey" damping factor (which will *not* necessarily be that of the Perey-Buck potential) is related directly to the elastic channel wronskian, a challenge for future work. Reference [22] provides an overview of the rationale for studying the nonlocal properties of the DPP and the significance of this nonlocality.

VIII. CONCLUSIONS

A. Summary of findings

We have extended the study of the influence of deuteron coupling on proton scattering to include coupling to the triton partition. Triton channels were included with various degrees of interaction with deuteron channels revealing a richness of phenomena that deserves further study. The present results, at 15.66, 25, and 61.3 MeV/nucleon, involved fitting the available experimental data, including some fits to transfer reactions that have been published previously [12]. The following results are specifically related to the atypical target nucleus ^{8}He; extension to more normal nuclei lies in the future.

(i) At each energy, the full (d5) coupling leads to a DPP with a repulsive real part, and a radial form resulting in a substantial reduction in the rms radius of the real potential. There is also a large absorptive term that leads to an increase in the rms radius of the imaginary potential.

(ii) Coupling to triton channels is important at the lowest energy but much less so at the highest energy. The triton channels by themselves have a repulsive/absorptive effect, yet reduce the similar effect of the deuteron channels alone. This was not significant at the highest energy, but its effect at 15.66 MeV/nucleon presents a challenge to our understanding.

(iii) The local DPPs were qualitatively similar at each energy, but the wavelength of the wavy features decreased with energy, as expected. The overall magnitudes of the real and imaginary DPPs are not small, even at the highest energy studied.

(iv) A clue to the nonlocality of the underlying DPP (to which we determine a local equivalent) lies in the nonadditivity of the local DPPs for partitions that are not mutually coupled. At 61.3 MeV/nucleon the additivity is nearly exact.

(v) Coupled deuteron channels have a substantial effect on the spin-orbit potential; coupled triton channels (transfer of a spin-zero neutron pair) do not. It would be of interest to study how the specific shell structure of different target nuclei influences the spin-orbit component of the DPP generated by pickup coupling.

B. Implictions for nucleon-nucleus interactions

The importance of coupled deuteron and triton channels shows that the scattering of nucleons from nuclei is not simply a problem of a single nucleon in the continuum. This raises the question of how this can be assimilated to experiment and phenomenology on the one hand and to formal theory on the other.

It is important to find evidence, based on fits to experimental data, for the effects that we have described. This requires precision fits to precise and wide angular range elastic-scattering data, including analyzing powers. This will not be easy for unstable target nuclei, making it difficult to establish the potentials unambiguously, but is possible in principle for stable nuclei. Because DPPs are not proportional to folding model potentials, model-independent fitting, either directly or as a modulation of a folding model potential, is required. Neither fits with standard parameterized forms, nor uniform renormalization of folding model potentials will capture the details necessary to verify the radial forms presented here. Moreover, CC processes are not an exhaustive source of "waviness" of nuclear potentials. It is known that the interaction of nucleons with light nuclei has a parity-dependent term arising from certain exchange processes (e.g., "heavy particle stripping") in the interaction with light nuclei. This has been shown for nuclear targets as heavy as ^{16}O and is quite substantial in the case of protons on ^{6}He [49]. The L-independent representation of this parity dependence leads to wavy potentials, complicating the analysis of elastic scattering or motivating precision fitting, according to one's point of view. To suggest what is involved, Fig. 11 shows the L-independent potential that precisely reproduces S_L (spin is ignored) for proton scattering from ^{8}He when S_L is calculated from the Koning and Delaroche [35] global potential in which the real term (only) has been multiplied by $[1.0 + 0.05(-1)^L]$. Note that the imaginary term as well as the real has a wavy component.

To assimilate the effects presented here into a comprehensive theory of nucleon scattering from nuclei is very challenging. As noted in subsection III C, it may be possible to incorporate the variation with Z, N, and E of the influence of reaction channels into a folding model theory as "shell

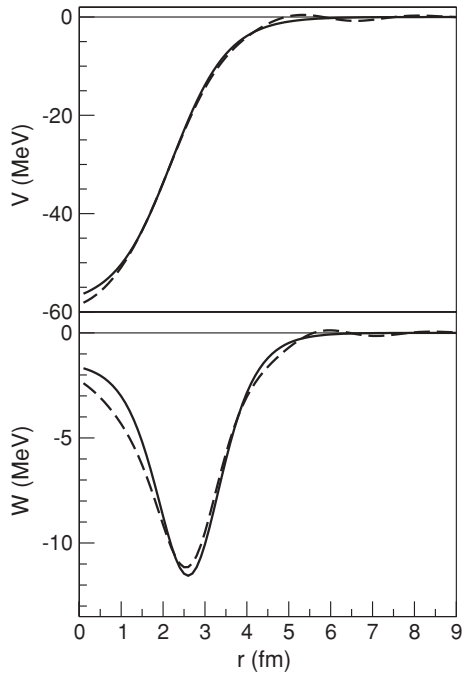

FIG. 11. Central potentials for protons, considered spinless, scattering elastically from ^{8}He at 15.66 MeV/nucleon. The solid line represents a smooth phenomenological potential to the real part of which a parity-dependent factor has been applied; the dashed line represents the L-independent potential found by inverting S_L from the parity-dependent potential.

corrections" analogous to the Strutinsky approach to nuclear masses.

C. What needs to be done

(i) How general is the reduction of the repulsive effect of (p, d) coupling by the addition of (p, t) coupling and the corresponding interpartition coupling? To answer this, similar calculations are required involving target nuclei that are less unusual than ^{8}He for which the pickup of a neutron pair may be unusually strong. This is important particularly in view of earlier demonstrations [10,11] of the contribution of (p, d) coupling to the real part of the nucleon OMP.

(ii) Inversion should be applied to new approaches to direct reaction theory, such as the development by Fonseca and Deltuva [50] and collaborators of practical implementations of the Faddeev formalism, providing an alternative to the CRC formalism. Unfortunately, the extension of such techniques to the d5 case is more difficult.

(iii) More generally, there is a need for the implementation of comprehensive antisymmetrized reaction theories that can handle both the reaction channel and the nuclear matter aspects of nucleon-nucleus scattering in a consistent way.

ACKNOWLEDGMENTS

R.S.M. is grateful to Valérie Lapoux for hospitality during the "Structure and Reactions in Coupled Reaction Channels" workshop of the ESNT at the CEA Saclay where this work was begun; R.S.M. and N.K. both acknowledge her inspirational encouragement and advice and also her calculation of the JLM potentials.

[1] R. S. Mackintosh, Phys. Lett. B **44**, 437 (1973); Nucl. Phys. A **230**, 195 (1974).
[2] R. S. Mackintosh and A. M. Kobos, Phys. Lett. B **62**, 127 (1976).
[3] C. A. Coulter and G. R. Satchler, Nucl. Phys. A **293**, 269 (1977).
[4] S. Kosugi and Y. Yoshida, Phys. Lett. B **106**, 353 (1981); Nucl. Phys. A **373**, 349 (1982).
[5] G. R. Satchler, *Direct Nuclear Reactions* (Clarendon Press, Oxford, 1983).
[6] I. J. Thompson, Comput. Phys. Rep. **7**, 167 (1988).
[7] V. I. Kukulin and R. S. Mackintosh, J. Phys. G **30**, R1 (2004).
[8] R. S. Mackintosh, A. A. Ioannides, and I. J. Thompson, Phys. Lett. B **178**, 1 (1986).
[9] S. G. Cooper, R. S. Mackintosh, and A. A. Ioannides, Nucl. Phys. A **472**, 101 (1987).
[10] F. Skaza, N. Keeley, V. Lapoux, N. Alamanos, F. Auger, D. Beaumel, E. Becheva, Y. Blumenfeld, F. Delaunay, A. Drouart, A. Gillibert, L. Giot, K. W. Kemper, R. S. Mackintosh, L. Nalpas, A. Pakou, E. C. Pollacco, R. Raabe, P. Roussel-Chomaz, J.-A. Scarpaci, J.-L. Sida, S. Stepantsov, and R. Wolski, Phys. Lett. B **619**, 82 (2005).
[11] R. S. Mackintosh and N. Keeley, Phys. Rev. C **76**, 024601 (2007).
[12] N. Keeley, F. Skaza, V. Lapoux, N. Alamanos, F. Auger, D. Beaumel, E. Becheva, Y. Blumenfeld, F. Delaunay, A. Drouart, A. Gillibert, L. Giot, K. W. Kemper, L. Nalpas, A. Pakou, E. C. Pollacco, R. Raabe, P. Roussel-Chomaz, K. Rusek, J.-A. Scarpaci, J.-L. Sida, S. Stepantsov, and R. Wolski, Phys. Lett. B **646**, 222 (2007).
[13] F. G. Perey and B. Buck, Nucl. Phys. **32**, 353 (1962).
[14] I. J. Thompson, M. A. Nagarajan, J. S. Lilley, and M. J. Smithson, Nucl. Phys. A **505**, 84 (1989).
[15] N. Keeley, J. S. Lilley, and J. A. Christley, Nucl. Phys. A **603**, 97 (1996).
[16] H. Feshbach, Ann. Phys. **5**, 357 (1958); **19**, 287 (1962).
[17] M. E. Brandon and G. R. Satchler, Phys. Rep. **285**, 143 (1997).
[18] F. G. Perey, in *Direct Interactions and Nuclear Reaction Mechanisms*, edited by E. Clemental and C. Villi (Gordon and Breach, New York, 1963), p. 125.
[19] D. F. Jackson and R. C. Johnson, Phys. Lett. B **49**, 249 (1974).
[20] R. S. Mackintosh, Nucl. Phys. A **164**, 398 (1971).
[21] C. L. Rao, M. Reeves, and G. R. Satchler, Nucl. Phys. A **207**, 182 (1973).
[22] G. H. Rawitscher, Nucl. Phys. A **475**, 519 (1987).
[23] W. G. Love, T. Terasawa, and G. R. Satchler, Phys. Rev. Lett. **39**, 6 (1977).
[24] A. J. Baltz, S. K. Kauffmann, N. K. Glendenning, and K. Pruess, Phys. Rev. Lett. **40**, 20 (1978).
[25] M. V. Andrés, J. Goméz-Camacho, and M. A. Nagarajan, Nucl. Phys. A **579**, 273 (1994); M. V. Andrés, J. A. Christley,

J. Goméz-Camacho, and M. A. Nagarajan, *ibid.* **625**, 685 (1997).
[26] R. S. Mackintosh, A. A. Ioannides, and S. G. Cooper, Nucl. Phys. A **483**, 173 (1988); **483**, 195 (1988).
[27] S. G. Cooper and R. S. Mackintosh, Nucl. Phys. A **511**, 29 (1990).
[28] M. A. Franey and P. J. Ellis, Phys. Rev. C **23**, 787 (1981).
[29] R. C. Braley and W. F. Ford, Phys. Rev. **182**, 1174 (1969).
[30] R. S. Mackintosh, Nucl. Phys. A **307**, 377 (1978).
[31] R. S. Mackintosh and S. G. Cooper, J. Phys. G: Nucl. Part. Phys. **23**, 565 (1997).
[32] J. P. Jeukenne, A. Lejeune, and C. Mahaux, Phys. Rev. C **16**, 80 (1977).
[33] B. A. Brieva and J. R. Rook, Nucl. Phys. A **291**, 299 (1977); **291**, 317 (1977); **297**, 206 (1978); **307**, 493 (1978).
[34] P. Navrátil and B. R. Barrett, Phys. Rev. C **57**, 3119 (1998).
[35] A. J. Koning and J. P. Delaroche, Nucl. Phys. A **713**, 231 (2003).
[36] R. V. Reid Jr., Ann. Phys. (NY) **50**, 441 (1968).
[37] A. K. Basak, O. Karban, S. Roman, G. C. Morrison, C. O. Blyth, and J. M. Nelson, Nucl. Phys. A **368**, 74 (1981).
[38] D. T. Khoa and W. von Oertzen, Phys. Lett. B **595**, 193 (2004).
[39] P. Guazzoni, L. Zetta, A. Covello, A. Gargano, G. Graw, R. Hertenberger, H.-F. Wirth, and M. Jaskola, Phys. Rev. C **69**, 024619 (2004).
[40] A. M. Eiró and I. J. Thompson, Phys. Rev. C **59**, 2670 (1999).
[41] R. Görgen, F. Hinterberger, R. Jahn, P. von Rossen, and B. Schüller, Nucl. Phys. A **320**, 296 (1979).
[42] R. Wolski, A. Pakou, and N. Alamanos, Yad. Fiz. **65**, 769 (2002) [Phys. At. Nucl. **65**, 736 (2002)].
[43] A. A. Korsheninnikov, E. Yu. Nikolskii, T. Kobayashi, A. Ozawa, S. Fukuda, E. A. Kuzmin, S. Momota, B. G. Novatskii, A. A. Ogloblin, V. Pribora, I. Tanihata, and K. Yoshida, Phys. Rev. C **53**, R537 (1996).
[44] M. Hatano *et al.*, Eur. Phys. J. A. **25**, 1, 255 (2005).
[45] V. N. Bragin, N. T. Burtebaev, A. D. Dujsebaev, G. N. Ivanov, S. B. Sakuta, V. I. Chuev, and L. V. Chulkov, Yad. Fiz. **44**, 312 (1986) [Sov. J. Nucl. Phys. **44**, 198 (1986)].
[46] R. S. Mackintosh and A. M. Kobos, Phys. Lett. B **116**, 95 (1982).
[47] A. A. Ioannides and R. S. Mackintosh, Nucl. Phys. A **467**, 482 (1987).
[48] N. Austern, Phys. Rev. **137**, B752 (1965).
[49] R. S. Mackintosh, Nucl. Phys. A **742**, 3 (2004).
[50] A. Deltuva and A. C. Fonseca, Phys. Rev. C **79**, 014606 (2009).